Table 2. Semiquantitative analysis for immunohistochemistry

	p62	*MATR3*	*TDP-43*	*ubiquitin*
VCPDM Case 1	++, aggregates	+, granular or loss of nuclear staining	++, aggregates	+, granular
VCPDM Case 2	++, aggregates	+, granular or loss of nuclear staining	±, diffuse	+, granular
sIBM	++, aggregates	±, granular	++, aggregates	+, granular
OPMD	++, aggregates	±, granular	++, aggregates	+, granular
GNE myopathy	++, aggregates	±, granular or loss of nuclear staining	+, aggregates	+, granular
VCP myopathy	++, aggregates	±, granular or loss of nuclear staining	++, aggregates	+, granular

VCPDM, vocal cord and pharyngeal weakness with distal myopathy; sIBM, sporadic inclusion body myositis; OPMD, oculopharyngeal muscular dystrophy.

-, no positive cells; ±, occasional positive cells; +, moderate numbers of positive cells; ++, frequent numbers of positive cells.

Figure legends

Figure 1. Muscle histology for the biopsy samples of VCPDM case 1 and 2.

(a–f) VCPDM case 1: (a, b) Hematoxylin and eosin (HE) staining at lower (a) and higher (b) magnifications. (c) Modified Gomori-trichrome staining. (d) Acid phosphatase staining. (e, f) ATPase staining at pH 10.6 (e), and pH 4.2 (f). I and II indicate type 1 and 2 fibers, respectively. Scale bars = 100 μm. (g–j) VCPDM case 2: (g, h) HE staining at lower (g) and higher (h) magnifications. (i) Acid phosphatase staining. (j–l) ATPase staining at pH 10.7 (j), pH 4.5 (k) and pH 4.2 (l). Scale bars = 200 μm (g, i), 50 μm (h) and 1.0 mm (j–l). (m, n) Electron microscopic analysis of samples from VCPDM case 1. Arrows indicate autophagic vacuoles. Scale bars = 500 nm (m), 800 nm (n).

Figure 2. Immunofluorescence studies for proteins related to myopathies with rimmed vacuoles.

Immunofluorescence study of p62 (green; a, e, i, m, q, u) and MATR3 (red; b, f, j, n, r, v) in identical specimens from VCPDM case 1 (a, b), case 2 (e, f), sIBM (i, j), OPMD (m, n), GNE myopathy with homozygous p.V572L mutation (q, r), and VCP myopathy with heterozygous p.A232E mutation (u, v). Double immunofluorescence study of TDP-43 (green) and MATR3

(red) in VCPDM case 1 (c), case 2 (g), sIBM (k), OPMD (o), GNE myopathy (s) and VCP myopathy (w). Double immunofluorescence study of p62 (green) and ubiquitin (red) in VCPDM case 1 (d), case 2 (h), sIBM (l), OPMD (p), GNE myopathy (t) and VCP myopathy (x). Double immunofluorescence study of phosphorylated TDP-43 (green) and LC-3 (red; 1: 500; Medical & Biological Laboratories, Nagoya, Japan) in VCPDM case 1(y). Immunolabeled proteins were visualized using anti-mouse immunoglobulin antibody-conjugated Alexa Fluor 488 or anti-rabbit immunoglobulin antibody-conjugated Alexa Fluor 594 (1: 200; Life Technologies Corporation, Carlsbad, CA, USA). Scale bars = 100 μm (a, b, e, f, m, n, q, r, u, v) and 50 μm (c, d, g, h, k, l, o, p, s, t, w, x, y). Nuclei were stained with 4', 6-diamidino-2-phenylindole (blue).

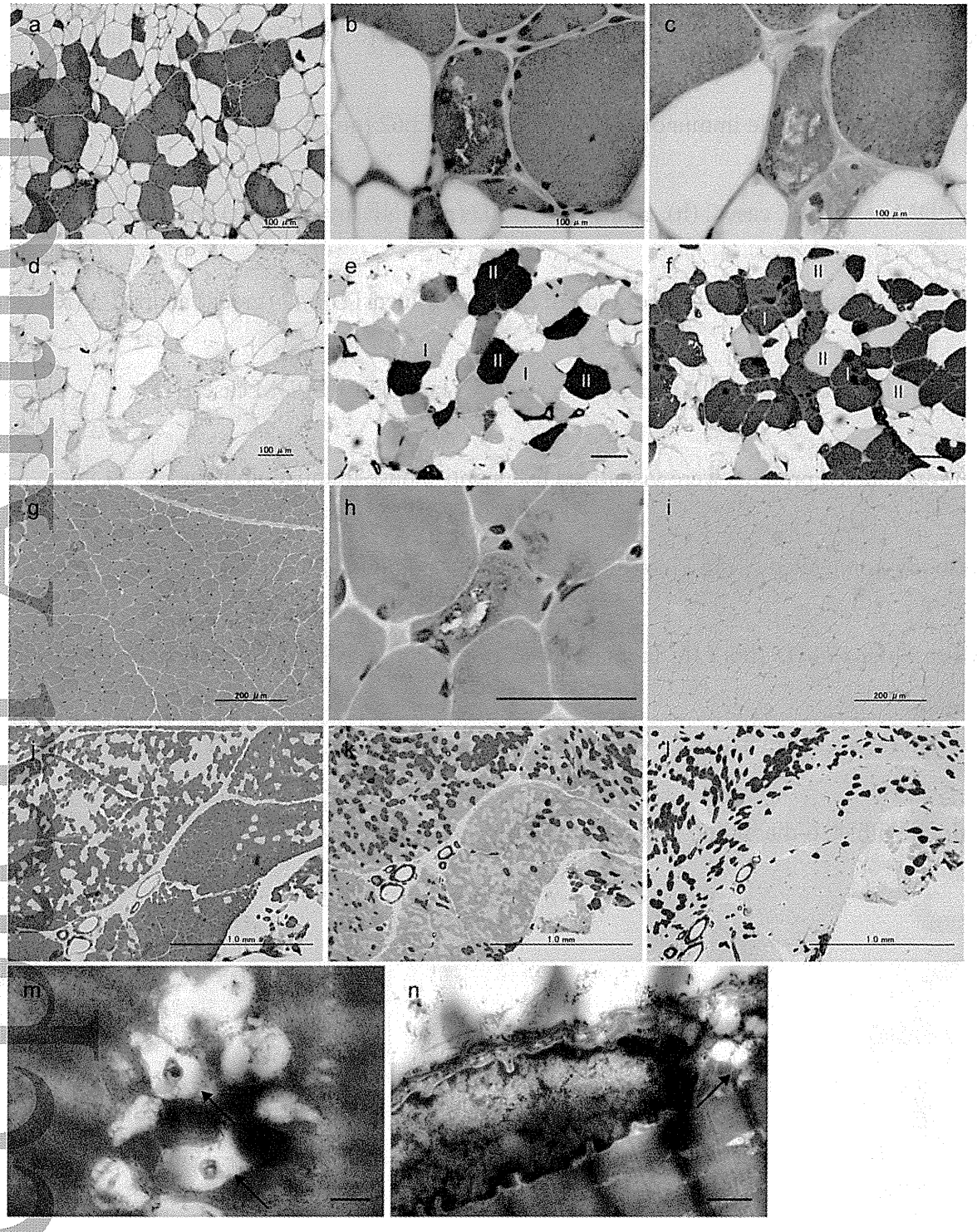

NAN_12179_F1

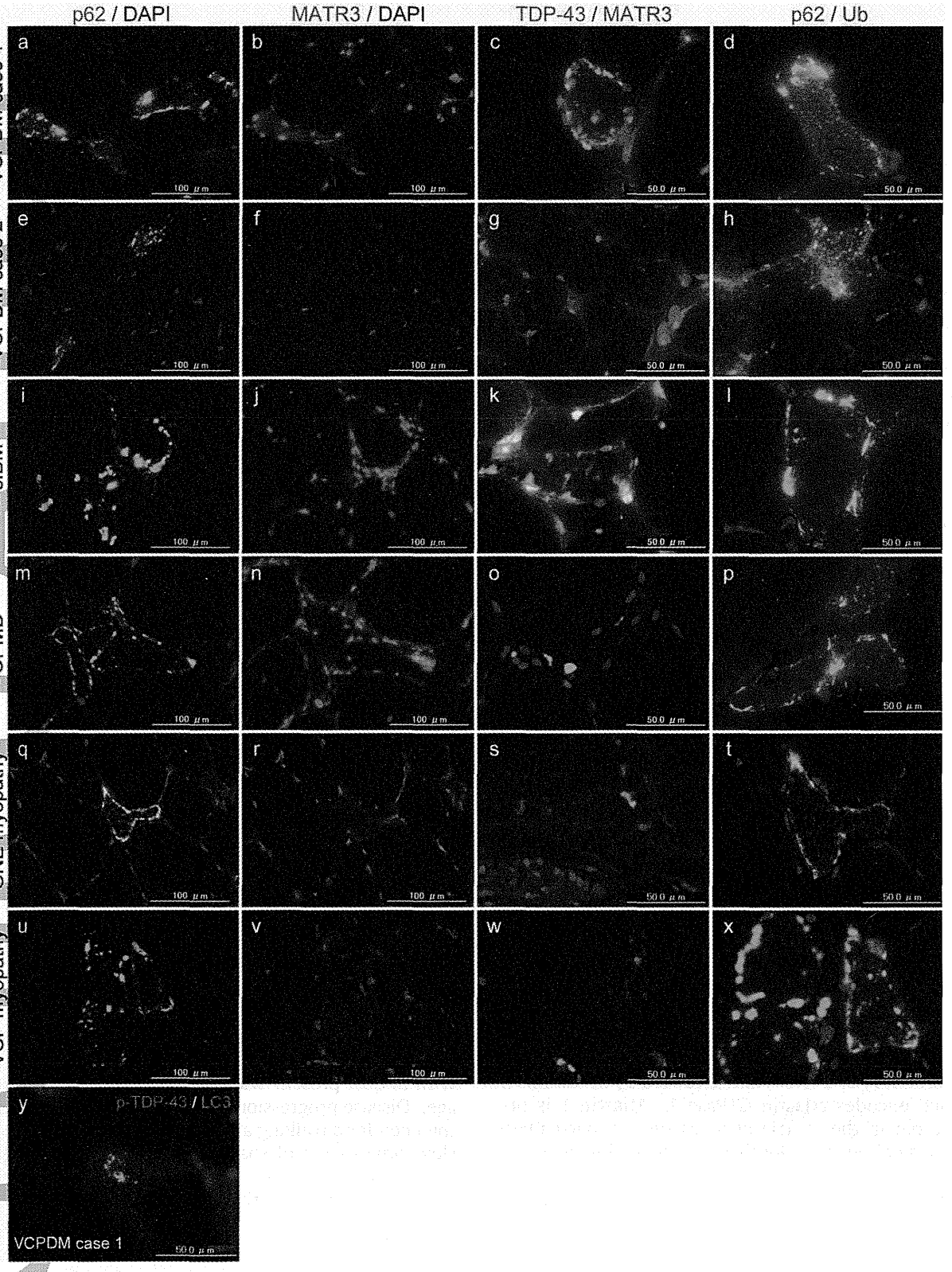

NAN_12179_F2

Pediatric Neurology 51 (2014) 726–729

Contents lists available at ScienceDirect

Pediatric Neurology

journal homepage: www.elsevier.com/locate/pnu

Clinical Observations

Extremely Severe Complicated Spastic Paraplegia 3A With Neonatal Onset

Takahiro Yonekawa MD, PhD [a,b,*], Yasushi Oya MD [c], Yujiro Higuchi MD [d], Akihiro Hashiguchi MD [d], Hiroshi Takashima MD, PhD [d], Kenji Sugai MD, PhD [a], Masayuki Sasaki MD, PhD [a]

[a] *Department of Child Neurology, National Center Hospital, National Center of Neurology and Psychiatry (NCNP), Tokyo, Japan*
[b] *Department of Neuromuscular Research, National Institute of Neuroscience, NCNP, Tokyo, Japan*
[c] *Department of Neurology, National Center Hospital, NCNP, Tokyo, Japan*
[d] *Department of Neurology and Geriatrics, Kagoshima University Graduate School of Medical and Dental Sciences, Kagoshima, Japan*

ABSTRACT

BACKGROUND: Spastic paraplegia 3A typically manifests in childhood as an uncomplicated form of hereditary spastic paraplegia with slow progression. Most affected individuals present with spasticity and weakness in the legs before the end of the first decade. **PATIENT:** We describe a 12-year-old boy with neonatal onset of extremely severe complicated spastic paraplegia 3A associated with a *de novo* c.1226G>A (p.G409D) mutation in *ATL1*, a gene which encodes atlatsin GTPase 1. He manifested general hypertonia and hypokinesia since the neonatal period and was initially diagnosed with cerebral palsy. He was never able to move without assistance because of severe spastic quadriplegia with distal dominant muscle weakness. He also developed with pseudobulbar palsy; his speech, chewing, and swallowing were severely impaired. Electrophysiological studies revealed severe diffuse axonal neuropathy. **CONCLUSIONS:** Extremely severe complicated spastic paraplegia 3A can be caused by mutations in the linker or three-helix bundle of atlastin 1.

Keywords: atlastin 1, spastic paraplegia, pseudobulbar palsy, axonal neuropathy

Pediatr Neurol 2014; 51: 726-729

Introduction

Spastic paraplegia (SPG) 3A is the second most common form of hereditary SPG (HSP) and is caused by mutations in *ATL1*, which encodes atlastin GTPase 1.[1] Atlastin 1 is primarily present in the central nervous system, particularly the corticospinal neurons, localized in the endoplasmic reticulum (ER) and *cis*-Golgi, and plays a role in ER and Golgi morphogenesis.[1,2] The mutation results in ER fusion defects, interference with correct membrane distribution or neuron polarity,[2,3] and axonal degeneration in the corticospinal tract neurons.

SPG3A usually manifests in childhood as uncomplicated HSP. The average age of onset is 4 years,[1] but infantile-onset SPG3A cases have also been documented.[4] Most patients with SPG3A present with a spastic gait before 10 years of age.[1] Disease progression is slow; wheelchair dependency or the need for a walking aid is relatively rare.[1] Early onset and slow progression of spasticity in the bilateral lower limbs mimic spastic diplegic cerebral palsy.[5] Moreover, complicated phenotypes with axonal neuropathy and/or distal amyotrophy have been observed. Here, we describe a 12-year-old boy with neonatal onset of an extremely severe complicated SPG3A phenotype associated with a novel *ATL1* mutation in the three-helix bundle domain of atlastin 1.

Patient Description

A 12-year-old boy with no family history of neuromuscular disease was evaluated for neonatal-onset severe spastic quadriplegia.

Article History:
Received March 27, 2014; Accepted in final form July 19, 2014

* Communications should be addressed to: Yonekawa; MD, PhD; Department of Child Neurology; National Center Hospital; NCNP; 4-1-1; Ogawa-Higashicho, Kodaira, Tokyo 187 8551, Japan.
E-mail address: yonekawa@ncnp.go.jp

0887-8994/$ - see front matter © 2014 Elsevier Inc. All rights reserved.
http://dx.doi.org/10.1016/j.pediatrneurol.2014.07.027

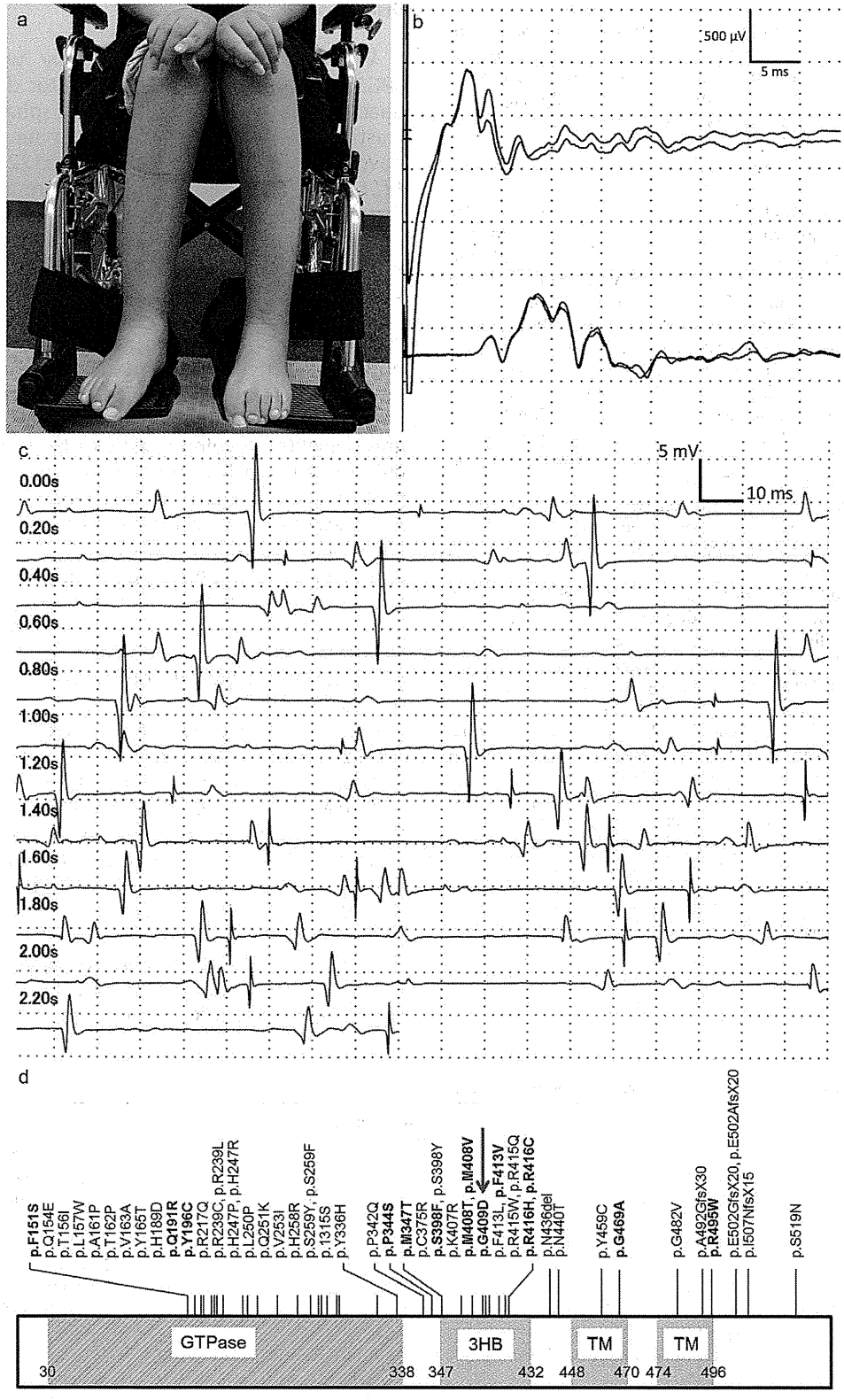

FIGURE.
Characteristic features of the patient (A-C). (A) The patient presents with muscle atrophy in all limbs, which is more pronounced distally and in the lower legs. (B) A nerve conduction study reveals right ulnar motor nerve responses evoked by stimuli of 25-33 mA. Surface stimulation of 0.2-ms duration was delivered through a two-pronged stimulator placed over the nerve at the wrist (upper) and elbow (bottom). Motor conduction velocity is not slowed (40.6 m/s). Compound muscle action potentials with temporal dispersion are decreased, suggesting diminished motor unit numbers. (C) Electromyography of the right tibialis anterior muscle revealed a chronic neurogenic pattern. (D) A schematic model of *ATL1* mutations in spastic paraplegia (SPG) 3A illustrates the distribution of SPG3A- or SPG-associated mutations and their amino acid residue changes.[4] Mutations (bold letters) associated with complicated phenotypes are more frequently present in the three-helix bundle of atlastin 1. Mutation locus of the patient is indicated with a red arrow. (Color version of this figure is available in the online edition.)

The parents were not consanguineous and were healthy, as was his younger brother. He was delivered uneventfully at 41 weeks of gestation. Lower limb hypertonia was evident in the neonatal period. Head control was achieved at 6 months of age. He could roll over at 2 years, but he could never sit unassisted. He was initially diagnosed with cerebral palsy. He presented with proximal hypertonia and distal hypotonia with markedly decreased voluntary movement. Oral baclofen and selective botulinum toxin injections provided no benefit.

He was referred to our hospital for diagnosis at 12 years of age. He presented with spastic quadriplegia and distal dominant muscle weakness and atrophy in all limbs (Figure A). Pes cavus was absent. Residual voluntary movement was markedly slowed, and fine hand movements were severely impaired. Eye movement and facial appearance were unaffected. Tongue movement was severely impaired, but atrophy and fasciculation were absent. Joint contracture was present at the shoulders, elbows, fingers, hips, and knees. Hyperreflexia of the orbicularis oculi, orbicularis oris, jaw, biceps brachii, brachioradialis, triceps brachii, and patellar reflexes was observed. The Achilles tendon reflex was absent, and the Babinski sign was not present. He could move himself from the supine to the lateral position with great difficulty and was unable to sit independently. He had dysarthria, dysphagia, and dysmasesis. Speech function was severely disturbed, but nonverbal intellect was well developed. There was no sphincter disturbance or scoliosis. Superficial and deep sensations were normal, and his condition was stable.

Nerve conduction studies revealed markedly decreased compound muscle action potentials with temporal dispersion, which were more pronounced in the lower limbs (Figure B). However, motor conduction velocity was intact (Table S1). Electromyography revealed proximal active denervation and a distal chronic neurogenic pattern (Figure C). Sensory nerve action potentials were decreased and absent in the upper and lower limbs, respectively (Fig S1 and Table S1). Severe diffuse axonal neuropathy and decreased motor units were observed. Computed tomography revealed symmetrical muscle atrophy and fat infiltration in the upper and lower limbs, particularly in the distal aspect, pelvis, and paraspinal region, suggesting a length-dependent peripheral axon abnormality (Fig S2). Brain magnetic resonance imaging was normal. There were no apparent abnormalities in auditory brainstem response. Exome sequencing revealed a heterozygous missense *ATL1* mutation, c.1226G>A (p.G409D), which was not listed in the 1000 Genome Project database or dbSNP 137. The p.G409D mutation was predicted to be damaging by the SIFT algorithm. This novel mutation was confirmed by conventional Sanger sequencing and was absent in the parents and sibling.

Discussion

We present a 12-year-old boy with neonatal-onset SPG3A that resulted in severe motor delay, severe spastic quadriplegia with dysarthria, dysphagia, distal muscle wasting, and axonal sensorimotor neuropathy. He had a novel *de novo* missense mutation, c.1226G>A (p.G409D) in *ATL1*. Dysarthria and dysphagia were attributed to axonal degeneration in the corticobulbar tracts because tongue movement was severely impaired and atrophy was absent, with hyperreflexia of the jaw reflex. Associated axonal predominantly motor neuropathy is observed in 17% SPG3A patients.[6] Distal muscle wasting in our patient reflected chronic motor axonopathy and decreased motor unit numbers. Therefore, markedly decreased spontaneous movement could cause multiple joint contractures.

SPG3A patients typically present with a pure form of HSP, and over 80% develop spasticity by 10 years of age.[1] Even children with early onset usually achieve ambulation, albeit with progressive gait disturbance.[7-9] Additional neurological features characterize complicated SPG3A: axonal neuropathy, distal muscle wasting, thin corpus callosum, and cerebellar involvement.[4] This child was never able to move without assistance because of severe spasticity in all limbs, with distal dominant muscle weakness and cranial nerve abnormalities. Extremely severe motor impairment and pseudobulbar palsy in our patient expand the known phenotypic spectrum of SPG3A.

Most published SPG3A- or SPG-associated mutations localize to the GTPase domain and three-helix bundle of atlastin 1 (Figure D).[4] Two mutations in *ATL1* (i.e., p.P344S and p.M408T) reportedly resulted in very early-onset (within 3 months of age) severe complicated SPG3A (Table).[10,11] The codons P344, M408, and G409 are located in the linker region or three-helix bundle of atlastin 1, providing a structural basis for dimerization and conformational changes in homotypic ER membrane fusion.[2,3] Other mutations responsible for complicated phenotypes are also frequent in the three-helix bundle (Figure D). This suggests that mutations in the linker or three-helix bundle

TABLE.
Characteristics of the Three Patients With Extremely Severe Complicated Spastic Paraplegia 3A

Items	17-yr-Old Girl[10]	7-yr-Old Boy[11]	Current Patient
Age at onset	3 mo	3 mo	Neonatal period
Symptom at onset	Axial hypotonia	Motor developmental delay	Hypertonia in the lower limbs
Maximal motor function	Unable to sit and walk	Sit and raise himself onto his knees	Roll over, unable to sit or walk
Spontaneous movement	Decreased	ND	Markedly decreased
Fine hand movement	ND	Severely impaired	Severely impaired
Intelligence	Moderate MR	Normal nonverbal intellect	Normal nonverbal intellect
Cranial nerve abnormalities	No speech, dysphagia, dysmasesis	Dysarthria, dysphagia	Dysarthria, dysphagia, dysmasesis
Muscle weakness	Severe	Severe	Severe
Muscle atrophy	Distal lower limbs, mild pes cavus	Four limbs, pronounced in distal lower limbs	Four limbs, pronounced in distal lower limbs
Deep tendon reflex	Brisk	Brisk, diffuse	Brisk, diffuse except in ATR
Pathological reflex	ND	+	−
Peripheral axonal neuropathy	+	+	+
ATL1 mutation	c.1030C>T (p.P344S)	c.1223T>C (p.M408T)	c.1226G>A (p.G409D)

Abbreviations:
ATR = Achilles tendon reflex
MR = Mental retardation
ND = Not described
"+" sign indicates presence and "−" indicates absence.

regions may have a major impact on altastin 1 function. The p.G409D mutation, as well as the p.P344S and p.M408T mutations, can be associated with the most severe form of SPG3A.

The authors are grateful to the patient and his family. They also acknowledge Takashi Iso of National Center of Neurology and Psychiatry and Akiko Yoshimura, BS of Kagoshima University for their excellent technical assistance. This study was supported, in part, by grants from the Nervous and Mental Disorders and Research Committee for Charcot-Marie-Tooth disease, neuropathy, ataxic disease, and Research on Applying Health Technology at the Japanese Ministry of Health, Welfare and Labour.

Supplementary Data

Supplementary data related to this article can be found at http://dx.doi.org/10.1016/j.pediatrneurol.2014.07.027.

References

1. Hedera P. Spastic paraplegia 3A. In: Pagon RA, Adam MP, Bird TD, et al. (ed) GeneReviews [Internet]. Seattle (WA): University of Washington, Seattle, 1993-2014. Available at: http://www.ncbi.nlm.nih.gov/books. Accessed March 24, 2014.
2. Byrnes LJ, Sondermann H. Structural basis for the nucleotide-dependent dimerization of the large G protein atlastin-1/SPG3A. *Proc Natl Acad Sci USA*. 2011;108:2216-2221.
3. Bian X, Klemm RW, Liu TY, et al. Structures of the atlastin GTPase provide insight into homotypic fusion of endoplasmic reticulum membranes. *Proc Natl Acad Sci USA*. 2011;108:3976-3981.
4. HGMD mutation result. Available at: http://portal.biobase-international.com/hgmd. Accessed February 14, 2014.
5. Rainier S, Sher C, Reish O, Thomas D, Fink JK. De novo occurrence of novel SPG3A/atlastin mutation presenting as cerebral palsy. *Arch Neurol*. 2006;63:445-447.
6. Ivanova N, Claery KG, Deconinck T, et al. Hereditary spastic paraplegia 3A associated with axonal neuropathy. *Arch Neurol*. 2007;64:706-713.
7. Dalpozzo F, Rossetto MG, Boaretto F, et al. Infancy onset hereditary spastic paraplegia associated with a novel atlastin mutation. *Neurology*. 2003;61:580-581.
8. Hedera P, Fenichel GM, Blair M, Haines JL. Novel mutation in the SPG3A gene in an African American family with an early onset of hereditary spastic paraplegia. *Arch Neurol*. 2004;61:1600-1603.
9. Fusco C, Frattini D, Farnetti E, et al. Hereditary spastic paraplegia and axonal motor neuropathy caused by a novel SPG3A de novo mutation. *Brain Dev*. 2010;32:592-594.
10. Fusco C, Frattini D, Farnetti E, Nicoli D, Casali B, Della Giustina E. Very early onset and severe complicated phenotype caused by a new spastic paraplegia 3A gene mutation. *J Child Neurol*. 2012;27:1348-1350.
11. Haberlová J, Claeys KG, Zámečník J, De Jonghe P, Seeman P. Extending the clinical spectrum of SPG3A mutations to a very severe and very early complicated phenotype. *J Neurol*. 2008;255:927-928.

Brief Clinical Note

A novel mutation in *glycyl-tRNA synthetase* caused Charcot-Marie-Tooth disease type 2D with facial and respiratory muscle involvement

Nobuko Kawakami, M.D.[1)2)], Kenichi Komatsu, M.D.[2)3)]*, Hirofumi Yamashita, M.D., Ph.D.[2)], Kengo Uemura, M.D., Ph.D.[2)4)], Nobuyuki Oka, M.D., Ph.D.[2)5)], Hiroshi Takashima, M.D., Ph.D.[6)] and Ryosuke Takahashi, M.D., Ph.D.[2)]

Abstract: BACKGROUND: Charcot-Marie-Tooth disease (CMT) is a hereditary peripheral neuropathy; symptoms include distal wasting and weakness, usually with some sensory impairment. The clinical course is typically benign and the disease is not life threatening; however, in some cases, severe phenotypes include serious respiratory distress. CASE REPORT: Here we describe a 45-year-old woman with a long course of motor-dominant neuropathy. Distal weakness appeared in childhood and became worse with age. After a diagnosis of CMT type 2, the symptoms progressed, and in her fourth decade, facial and respiratory muscle weakness appeared, ultimately requiring non-invasive mechanical ventilation. There was no family history of CMT. Comprehensive analysis of known CMT-related genes revealed a novel heterozygous c.815T>A, p.L218Q mutation in *glycyl-tRNA synthetase* (*GARS*), a causative gene for both CMT type 2D (CMT2D) and distal spinal muscular atrophy type V (dSMA-V). This mutation was considered pathogenic based on molecular evidence; notably, it was unique in that all other reported *GARS* mutations associated with severe phenotypes are located in an anticodon-binding domain, while in this case in an apparently non-functional region of the *GARS* gene. Not a simple loss-of-function mechanism, but rather gain-of-function mechanisms have also been reported in *GARS* mutations. This case provided useful information for understanding the mechanism of CMT2D/dSMA-V.

(Clin Neurol: 2014;54:911-915)

Key words : Charcot-Marie-Tooth disease, hereditary sensory and motor neuropathy, glycine-tRNA ligase, spinal muscular atrophy, respiratory distress

Introduction

Charcot-Marie-Tooth disease (CMT) is a hereditary peripheral neuropathy presenting distal wasting and weakness, usually with some distal sensory impairment. In most cases, the clinical course is benign and the disease is not life threatening; however, in some cases, severe phenotypes can include respiratory distress, which, in relation to adults, is not widely recognized in the literature[1)]. We describe a unique case characterized by progression of serious symptoms; ultimately, these included facial and respiratory muscle impairment, and a novel mutation was found in the *glycyl-tRNA synthetase* gene (the gene is abbreviated as *GARS* and the protein as GlyRS), which is a causative gene for both CMT type 2D (CMT2D) and distal spinal muscular atrophy type V (dSMA-V).

Case report

A 45-year-old woman initially presented with distal dominant muscle atrophy, which progressed, and facial muscle atrophy and

*Corresponding author: Department of Neurology, Kitano Hospital, The Tazuke Kofukai Medical Research Institute〔2-4-20 Ohgimachi, Kita-ku, Osaka-shi, Osaka 530-8480〕

[1)]Department of Neurology, Shizuoka General Hospital

[2)]Department of Neurology, Kyoto University Graduate School of Medicine

[3)]Department of Neurology, Kitano Hospital, The Tazuke Kofukai Medical Research Institute

[4)]Ishiki Hospital

[5)]Department of Neurology, National Hospital Organization Minami Kyoto Hospital

[6)]Department of Neurology and Geriatrics, Kagoshima University Graduate School of Medical and Dental Sciences

(Received: 14 January 2014)

respiratory failure developed subsequently. The patient was born after 32 weeks of gestation without any abnormality. Walking was slightly delayed and running speed was slow through her preschool years. Bilateral foot drop developed around age 7, and distal muscle atrophy developed in all limbs by age 10. She was wheelchair-bound in her third decade. At age 29, she was admitted to our hospital for three months; muscle and nerve biopsies were performed, and she subsequently received a diagnosis of CMT type 2 (CMT2) with evidence of axonal sensorimotor neuropathy. At age 36, respiratory muscle dysfunction developed and non-invasive mechanical ventilation was started. At age 45, she was admitted for re-evaluation. Her parents were unrelated to one another (Fig. 1A). Her mother had died at age 46 due to unknown causes. Her father and brother were alive and healthy at the writing of this report. Physical examination showed severe atrophy in all skeletal muscles, including limb, truncal, facial and tongue muscles (Fig. 1B). Dysphagia and nasal voice were evident. Her muscle strength scores, which were based on the Medical Research Council scale, were 2 out of 5 for proximal muscles and 1 out of 5 for distal muscles. Deep tendon reflexes were absent. Sensory disturbance was mild and only evident with distal lower limbs.

In nerve conduction studies, compound muscle action potentials (CMAPs) were not evoked from routinely examined muscles, including the abductor pollicis brevis, abductor digiti minimi and flexor hallucis brevis. CMAPs from the flexor carpi radialis had extremely low amplitudes, but the distal latency was normal, and conduction velocities were only slightly decreased (42 m/s) relative to normal values. Sensory nerve action potentials (SNAPs) and sensory conduction velocities (SCVs) from the median nerve were normal. SNAPs from the sural nerve had been recorded when the patient was 29 years old; these SNAPs had very low amplitudes (2.1 μV), but the SCVs were normal (55 m/s). Needle electromyography showed chronic neurogenic patterns.

A muscle biopsy from triceps brachii was performed at age 29. The majority of the muscle fibers ranged from 70 to 100 μV in diameter. Pyknotic clamp was present in the rim of a fascicle. Necrotic or regenerating fibers were not observed. Islands of groups of extremely atrophic fibers and spindles were present in epimysium. Internal nuclei were moderately increased. Muscle fibers occasionally showed fiber splitting. Fatty connective tissue was increased in perimysium and more markedly in epimysium. Trichrome staining added no information. Intermyofibrillar network was preserved in NADH dehydrogenase-stained sections. Every fascicle of fibers showed fiber-type grouping as assessed by ATPase staining. These findings were consistent with chronic denervation.

A sural nerve biopsy also taken at age 29 revealed moderate loss of myelinated fibers; however, axonal degeneration and active demyelination were not evident. Perivascular mononuclear cells were observed in epineurium, but these cells had not infiltrated the endoneurium. Substantial deposition of fat droplets was observed at the tunica media-externa of small arteries (Fig. 1C). Electron microscopy revealed no obvious mitochondrial abnormalities.

Lung CT scan revealed no abnormalities. Electrocardiogram showed normal sinus rhythm with a tall P wave and right axis deviation. Echocardiogram appeared normal.

A comprehensive sequence analysis of CMT-related genes[2)3)] revealed a novel heterozygous c.815T>A, p.L218Q mutation in the *GARS* gene (Fig. 1D). The patient's unaffected father and brother did not carry this mutation. HomoloGene (http://www.ncbi.nlm.nih.gov/homologene) was used to conduct a sequence homology search; we found that leucine 218 in GlyRS was highly conserved among species (Fig. 1E). The computational protein function-predicting algorithm MUPro score was −1; this value indicated that the mutant protein was less stable than the wild-type protein (http://www.igb.uci.edu/~baldig/mutation.html). Moreover, the Polyphen-2 score was 1.0; this score indicated that the mutant GlyRS protein was pathogenic (http://genetics.bwh.harvard.edu/pph2/).

Discussion

We present a unique case of CMT that involved a new mutation in *GARS*; the patient initially developed moderate CMT2 symptoms and subsequently developed facial and respiratory muscle impairment.

GARS is one of 37 *aminoacyl-tRNA synthetases (ARSs)*. *ARSs* are divided into two groups, based upon their cytoplasmic or mitochondrial localization. Among them, *GARS* and *lysyl-tRNA synthetase (KARS)* are localized to both the cytoplasm and mitochondria. GlyRS, the product protein of *GARS* gene, is ubiquitously expressed, including the brain and spinal cord[4)]. It has two isoforms, with and without an N-terminal mitochondrial targeting sequence (MTS), localizing in the mitochondria and cytoplasm, respectively. GlyRS catalyzes attachment of glycine to its cognate tRNA for protein synthesis and non-translational functions of GlyRS include tumor suppression when secreted[5)6)]. Remarkably, all known disease-associated mutations in cytoplasmic *ARSs* are associated with CMT and related neuropathies, and the causative genes include *GARS*, *KARS*, *tyrosyl-tRNA synthetase (YARS)*, and *alanyl-tRNA synthetase (AARS)*[6)]. *GARS* is also one of the genes that, when mutant, can cause CMT2 or distal spinal muscular atrophy (dSMA)[3)]; conditions originating from *GARS* mutations are called CMT2D or dSMA-V, depending on whether sensory nerves are affected. The majority of previously reported CMT2D/dSMA-V cases involved adolescent onset with upper limb-dominant weakness, and the progression of symptoms was slow[4)7)~12)]. Other organs including brain and

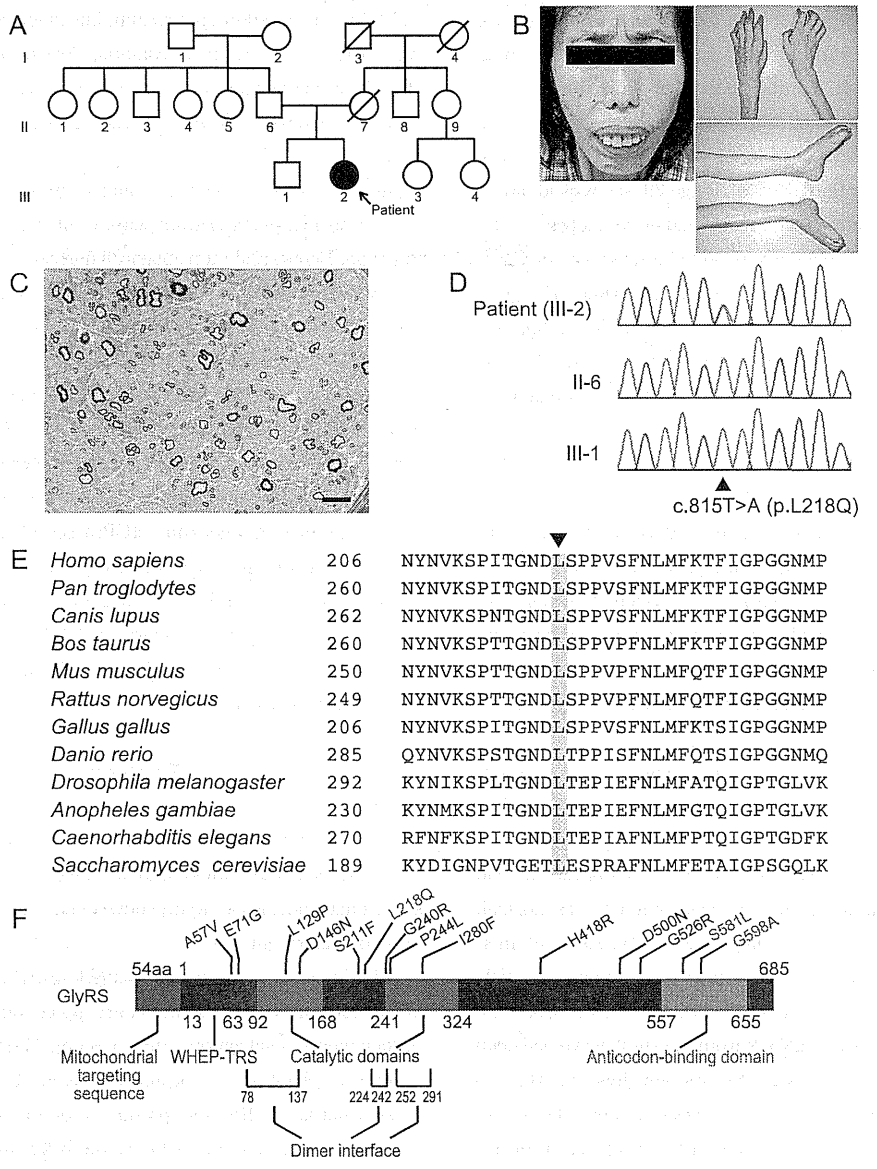

Fig. 1 Clinical, pathological and molecular features of the patient.

(A) Pedigree. (B) Facial involvement with weakness of the orbicularis oris and atrophy of the temporalis and masseter muscles. The patient was instructed to close her mouth. Limbs showed severe muscle atrophy. (C) The sural nerve biopsy at age 29 showed moderate loss of myelinated fibers. Axonal degeneration and active demyelination were not evident. Bar = 20 μm. (D) Chromatogram of the heterozygous c.815T>A (p.L218Q) mutation in exon 7 of *GARS*; the patient and two unaffected relatives. (E) Comparison of GlyRS from different species. Arrowhead on top of the alignment indicates amino acid position 218 (Note: numbering differences from related species are because the human annotation does not consider the N-terminal mitochondrial targeting sequence appended through alternative start codon usage). (F) The GlyRS protein contains four functional domains and three dimer interface regions. Mutations identified in GlyRS are distributed across the entire protein; modified from Motley, et al[13]. L218Q, the mutation found in our patient is shown in purple. It is located in an apparently non-functional region. In contrast, both of two other known mutations that cause early onset and severe clinical phenotypes, shown in red, are located in an anticodon-binding domain.

muscle were not involved. Even though mitochondrial isoform of GlyRS localizes in mitochondria, mitochondrial disorders like myopathy and MELAS are not reported in GlyRS mutations, unlike mutations of other mitochondrial ARSs[6]. Neither muscle or nerve biopsy in the presented case showed mitochondrial abnormalities.

Table 1 *In silico* analysis of previously reported mutations.

Authors	Domains	Mutations	MUPro		Polyphen-2
			Method 1	Method 2	
Rohkamm, *et al.* (2007)[8]	WHEP-TRS	A57V	−0.13	−0.76	0.439
Antonellis, *et al.* (2003)[4]		E71G	−0.76	−0.98	0.788
Antonellis, *et al.* (2003)[4]	Catalytic-1	L129P	−1.00	−1.00	1.000
Lee, *et al.* (2012)[9]		D146N	−0.79	−0.86	1.000
Lee, *et al.* (2012)[9]		S211F	0.19	0.55	1.000
Presented case		L218Q*	−1.00	−0.96	1.000
Antonellis, *et al.* (2003)[4]		G240R	0.30	0.68	1.000
Abe, *et al.* (2009)[10]	Catalytic-2	P244L	0.25	0.67	1.000
James, *et al.* (2006)[7]		I280F	−1.00	−1.00	1.000
Sivakumar, *et al.* (2005)[11]		H418R	0.55	0.73	0.998
Del Bo, *et al.* (2006)[12]		D500N	−0.53	−0.79	0.048
Antonellis, *et al.* (2003)[4]		G526R	0.01	−0.51	1.000
James, *et al.* (2006)[7]	Anticodon-binding	S581L*	0.15	0.80	0.420
James, *et al.* (2006)[7]; Eskuri, *et al.* (2012)[14]		G598A*	0.86	0.82	0.013

Asterisks indicate mutations associated with severe phenotypes. MUPro scores range between −1 and 1. A score less than 0 means that the mutation decreases the protein stability, and *vice versa*. A larger absolute value indicates more confident prediction. Polyphen-2 scores range between 0 and 1. A larger score indicates that the mutation is more pathogenic. Underlines indicate high scores, predicting unstability and pathogenicity of the mutated proteins.

The GlyRS protein comprises four functional domains and three dimer interface regions[13] (Fig. 1F). (Note: numbering of residues starts from the alternative start codon after MTS in human protein). Among 13 reported *GARS* mutations[7–10,14], two mutations caused early-onset clinical phenotypes in four patients. One patient developed facial and respiratory muscle involvement[7], and another developed vocal cord dysfunction[14]. Both mutations are located in an anticodon-binding domain. In contrast, the mutation described in the current study was located in neither of the functional domains. Even so, we still consider this L218Q mutation a pathogenic mutation based on the following reasons: 1) its close location to the dimer interface region; 2) the high conservation of the affected amino acid; and 3) the fact that neither the unaffected parent nor the unaffected brother carried this mutation. *In silico* prediction using MUPro and Polyphen-2 suggests pathogenicity of the mutation, but the results from other reported mutations using these algorithms do not necessarily correlate with clinical severity (Table 1) and this approach may not be suitable as far as this gene is concerned.

Mechanisms underlying CMT2D/dSMA-V caused by *GARS* mutations have been examined from various aspects, including enzyme activity, protein stability and dimerization, but those properties considerably depend on individual mutations and none of these approaches reached consistent results. Moreover, heterozygous mice with a single loss-of-function *GARS* allele exhibited reduced synthetase activity but none of the symptoms of CMT[15] and overexpression of wild-type GlyRS could not rescue the neuropathy phenotype in mouse models[16]. These experimental results, together with the observations of scattered locations of the mutations throughout the gene and the dominant inheritance pattern lead to a consequence that not a simple loss-of-function, but rather a gain-of-function mechanism significantly contributes to the pathogenesis of the disease[5,6,13]. Recent study analyzing the tertiary structure of GlyRS using hydrogen-deuterium exchange revealed that all five mutations tested promote the same localized conformational opening[17]. All other mutations untested are also within the opened-up areas, except for some mutations which are not covered in that analysis. They argued that those opened-up areas provide unique surfaces for potential novel interactions that lead to pathological consequences. The mutation of our case is also within the "opened-up areas" and that may account for the pathogenicity.

Although both loss-of-function and gain-of-function mechanisms were likely to synergistically give rise to severe phenotypes in the previous cases with mutations in an anticodon-binding domain, gain-of-function predominantly appears to have led to severe phenotypes in our case. Data from this unique case provided new information for understanding the mechanism of CMT2D/dSMA-V and for drug discovery as well.

The patient and family members included in this study gave written informed consent, and the study was approved by the Kyoto University and the Institutional Review Board of Kagoshima University.

Abstract of this work was presented at the 98th Kinki Regional Meeting of the Japanese Society of Neurology and recommended by the conference chairperson for the publication to Rinshō Shinkeigaku.

Acknowledgment: The authors wish to thank the patient and the family described in this report for their cooperation, Dr. Y. Takahashi for sample preparation and study coordination, Dr. S Nakano for the pathological analysis of the muscle biopsy and Dr. Y. Higuchi and Dr. A. Hashiguchi for the molecular analysis.

※ The authors declare there is no conflict of interest relevant to this article.

References

1) Wilmshurst JM, Ouvrier R. Hereditary peripheral neuropathies of childhood: an overview for clinicians. Neuromuscul Disord 2011;21:763-775.
2) Takashima H. Genetic diagnosis and molecular pathology of inherited neuropathy. Rinsho Shinkeigaku 2012;52:399-404.
3) Zhao Z, Hashiguchi A, Hu J, et al. Alanyl-tRNA synthetase mutation in a family with dominant distal hereditary motor neuropathy. Neurology 2012;78:1644-1649.
4) Antonellis A, Ellsworth RE, Sambuughin N, et al. Glycyl tRNA synthetase mutations in Charcot-Marie-Tooth disease type 2D and distal spinal muscular atrophy type V. Am J Hum Genet 2003;72:1293-1299.
5) Guo M, Schimmel P. Essential nontranslational functions of tRNA synthetases. Nat Chem Biol 2013;9:145-153.
6) Yao P, Fox PL. Aminoacyl-tRNA synthetases in medicine and disease. EMBO Mol Med 2013;5:332-343.
7) James PA, Cader MZ, Muntoni F, et al. Severe childhood SMA and axonal CMT due to anticodon binding domain mutations in the GARS gene. Neurology 2006;67:1710-1712.
8) Rohkamm B, Reilly MM, Lochmüller H, et al. Further evidence for genetic heterogeneity of distal HMN type V, CMT2 with predominant hand involvement and Silver syndrome. J Neurol Sci 2007;263:100-106.
9) Lee HJ, Park J, Nakhro K, et al. Two novel mutations of GARS in Korean families with distal hereditary motor neuropathy type V. J Peripher Nerv Syst 2012;17:418-421.
10) Abe A, Numakura C, Saito K, et al. Neurofilament light chain polypeptide gene mutations in Charcot-Marie-Tooth disease: nonsense mutation probably causes a recessive phenotype. J Hum Genet 2009;54:94-97.
11) Sivakumar K, Kyriakides T, Puls I, et al. Phenotypic spectrum of disorders associated with glycyl-tRNA synthetase mutations. Brain 2005;128:2304-2314.
12) Del Bo R, Locatelli F, Corti S, et al. Coexistence of CMT-2D and distal SMA-V phenotypes in an Italian family with a GARS gene mutation. Neurology 2006;66:752-754.
13) Motley WW, Talbot K, Fischbeck KH. GARS axonopathy: not every neuron's cup of tRNA. Trends Neurosci 2010;33:59-66.
14) Eskuri JM, Stanley CM, Moore SA, et al. Infantile onset CMT2D/dSMA V in monozygotic twins due to a mutation in the anticodon-binding domain of GARS. J Peripher Nerv Syst 2012; 17:132-134.
15) Seburn KL, Nangle LA, Cox GA, et al. An active dominant mutation of glycyl-tRNA synthetase causes neuropathy in a Charcot-Marie-Tooth 2D mouse model. Neuron 2006;51:715-726.
16) Motley WW, Seburn KL, Nawaz MH, et al. Charcot-Marie-Tooth-linked mutant GARS is toxic to peripheral neurons independent of wild-type GARS levels. PLoS Genet 2011;7: e1002399.
17) He W, Zhang HM, Chong YE, et al. Dispersed disease-causing neomorphic mutations on a single protein promote the same localized conformational opening. Proc Nat Acad Sci USA 2011;108:12307-12312.

平成26年度厚生労働科学研究委託費

難治性疾患等克服研究事業 難治性疾患等実用化事業(難治性疾患実用化研究事業)

「シャルコー・マリー・トゥース病の診療向上に関するエビデンスを構築する研究
(H26-委託(難)－一般－071)」班(CMT研究班)
(研究代表者　京都府立医科大学附属北部医療センター　中川正法)
平成26年度第1回班会議
平成26年8月31日(日)10:00～11:30　京都ホテルオークラ

議題

1. 研究費の経理処理について
   今後の提出について(山崎)
   研究報告書類・経理報告書類　資料

2. 班員の自己紹介
   別紙1

3. 今後の研究の進め方　(中川)
   別紙2

4. CMT患者登録システムについて
   富士通(株)の島田理生様

5. CMT市民公開講座
   平成26年11月9日(日)鹿児島会場　13：00～16：00
   プラザN4F　ヴァリエホール
   鹿児島市武1-4-2(JR鹿児島中央駅西口より徒歩3～5分)
   TEL 099-298-1000、http://www.plaza-n.com/varierhall/

   平成26年12月7日(日)名古屋会場14：00～17：00
   ミッドランドホール5F　会議室A(JR名古屋駅より徒歩5分)
   〒450-6025　名古屋市中村区名駅四丁目7番1号
   ミッドランドスクエア　オフィスタワー5F
   TEL 052-527-8500　http://www.midland-hall.com/

   平成27年1月18日(日)東京会場14：00～16：30
   東京ステーションコンファレンス　502班会議　　503公開講座
   〒100-0005東京都千代田区丸の内1-7-12　サピアタワー5F

TEL　03-6888-8080（代表）〒450-6025

6. 第２回班会議

研究分担者の先生方にご発表頂きます。

平成27年1月18日（日）班会議　10：00～12：00
東京ステーションコンファレンス　502班会議
〒100-0005東京都千代田区丸の内1-7-12　サピアタワー5F
TEL　03-6888-8080（代表）〒450-6025

7. International Hereditary Neuropathy Symposium in Kyoto　別冊

Satellite Symposium of 25th Annual meeting of Japanese Peripheral Nerve Society
"New era of Hereditary Neuropathy"
August 31, 2014
0:50pm to 6pm, at Kyoto Hotel Okura, 3rd floor, Room Kongo.
Buffet-style dinner party at Apollon 17th floor, Kyoto Hotel Okura

8. その他

CMT の難病指定の可能性

認定基準（案）別紙３

本研究に関連する論文発表の際には、本研究事業についての謝辞を必ず記載してください。
＜英文例＞

This work was supported by Grants-in-Aid from the Research Committee of Charcot-Marie-Tooth Disease, the Ministry of Health, Labour and Welfare of Japan.

＜和文例＞

この研究は厚生労働科学研究費補助金（難治性疾患克服研究事業）「シャルコー・マリー・トゥース病の診療向上に関するエビデンスを構築する研究 」によっておこなわれた。

＜メモ＞

平成26年度厚生労働科学研究委託費

難治性疾患等克服研究事業　難治性疾患等実用化事業(難治性疾患実用化研究事業)

「シャルコー・マリー・トゥース病の診療向上に関するエビデンスを構築する研究

(H26-委託（難）－一般－071）」班（CMT研究班)

(研究代表者　京都府立医科大学附属北部医療センター　中川正法)

平成26年度第2回班会議

平成27年1月18日（日）10:00～12:00　東京ステーションコンファレンス

議題

1. 研究費の経理処理について

今後の提出について（山崎)

研究報告書類・経理報告書類　資料

2. 分担研究発表（演題名、ご所属、演者、研究分担者)

演題１．Charcot-Marie-Tooth 病の包括的遺伝子診断

鹿児島大学医歯学総合研究科　神経内科・老年病学講座

●橋口昭大　　髙嶋　博

演題２．常染色体劣性軸索型または中間型 Charcot-Marie-Tooth（CMT)における *COX6A1* 変異

山形大学医学部小児科学講座

●阿部　暁子

演題３．Charcot-Marie-Tooth（CMT）病の発症と関連する変異 PMP22 の小胞体蓄積機構の解析

群馬大学生体調節研究所細胞構造分野

●原　太一

演題４．Charcot-Marie-Tooth 病に伴う足部変形に対する手術治療

名古屋市立大学リハビリテーション医学分野

●和田郁雄

演題５．シャルコー・マリー・トゥース病の下肢装具選定の指標作成に向けて

国立精神・神経医療研究病院身体リハビリテーション科

●小林庸子、矢島寛之

演題６．Charcot-Marie-Tooth 病の障害像

産業医科大学リハビリテーション医学

●松嶋康之

演題 7．Charcot-Marie-Tooth Patient Registry (CMTPR) システム構築

京都府立医科大学大学院・総合医療・医学教育学　滋賀　健介
神経内科学　能登　祐一、辻　有希子
京都府立医科大学附属北部医療センター
●中川　正法

3. 今後の研究の進め方　(中川)

4. CMT 患者登録システムについて
富士通（株）様　別紙資料

5. その他

本研究に関連する論文発表の際には、本研究事業についての謝辞を必ず記載してください。
＜英文例＞
This work was supported by Grants-in-Aid from the Research Committee of Charcot-Marie-Tooth Disease, the Ministry of Health, Labour and Welfare of Japan.

＜和文例＞
この研究は厚生労働科学研究費補助金（難治性疾患克服研究事業）「シャルコー・マリー・トゥース病の診療向上に関するエビデンスを構築する研究 」によっておこなわれた。

＜メモ＞

シャルコー・マリー・トゥース病（CMT）市民公開講座

皆さん、「CMT」ってご存じですか？
シャルコー・マリー・トゥース病という病気の略語です。「CMT」は，末梢神経が障害される疾患の総称です．CMT 患者さんの多くは，足や手の先の筋肉がゆっくりと進行性に痩せていく、痛みや冷たさに対する手足の感覚が鈍くなる病気です．私たちは厚生労働省の科学研究補助金 を受けて、「シャルコー・マリー・トゥース病の診断・治療・ケアに関する研究」を行っております。その一環として、市民の皆様に「CMT」に対するご理解を深めて頂きたいと考え、今回の市民公開講座を企画致しました。一人でも多くの市民の皆様のご参加をお持ちしております。

日時：平成 26 年 11 月 9 日（日）　　13：30-16：00

会場：プラザＮ　４Ｆ　ヴァリエホール

入場無料

―講演内容―

主催者あいさつ	中川正法
CMT 病の研究の動向	中川正法
CMT の手術療法と術後後療法＆痛みとしびれの対処法	中川正法（渡邉耕太）
CMT 病の病態と治療・ケアおよび研究の現状	高嶋　博
CMT 病のリハビリテーション	松嶋康之
CMT 病患者を対象とした自己記入式アンケート調査	滋賀健介
日常生活と工夫、社会資源の利用	宮口琢磨（大竹弘哲）
CMT 友の会～その活動について～	山田隆司
質疑応答	中川正法

主催

平成２６年度厚生労働科学研究委託事業
（難治性疾患等克服研究事業（難治性疾患等実用化研究事業（難治性疾患実用化研究事業）））
「シャルコー・マリー・トゥース病の診療向上に関するエビデンスを構築する研究」（CMT研究班）
（研究代表者　京都府立医科大学附属北部医療センター　病院長　中川正法）

シャルコー・マリー・トゥース病（CMT）市民公開講座

皆さん、「CMT」ってご存じですか？
シャルコー・マリー・トゥース病という病気の略語です。「CMT」は，末梢神経が障害される疾患の総称です．CMT 患者さんの多くは，足や手の先の筋肉がゆっくりと進行性に痩せていく、痛みや冷たさに対する手足の感覚が鈍くなる病気です．私たちは厚生労働省の科学研究補助金 を受けて、「シャルコー・マリー・トゥース病の診断・治療・ケアに関する研究」を行っております。その一環として、市民の皆様に「CMT」に対するご理解を深めて頂きたいと考え、今回の市民公開講座を企画致しました。一人でも多くの市民の皆様のご参加をお持ちしております。

日時：平成 26 年 12 月 7 日（日）　14：00-16：30

会場：　ミッドランドスクエア オフィスタワー５F

入場無料

―講演内容―

主催者あいさつ	中川正法
CMT 病の研究の動向	中川正法
CMT 病の病態と治療・ケアおよび研究の現状	高嶋　博
CMT 病のリハビリテーション	松嶋康之
―　休憩　―	
CMT による下肢障害と対応	和田郁雄
CMT 病患者を対象とした自己記入式アンケート調査	滋賀健介
日常生活と工夫、社会資源の利用	大竹弘哲
CMT 友の会～その活動について～	山田隆司
質疑応答	中川正法

主催

平成２６年度厚生労働科学研究委託事業
（難治性疾患等克服研究事業（難治性疾患等実用化研究事業（難治性疾患実用化研究事業）））
「シャルコー・マリー・トゥース病の診療向上に関するエビデンスを構築する研究」（CMT研究班）
（研究代表者　京都府立医科大学附属北部医療センター　病院長　中川正法）